Global Solar Wind Model with Physics-based Alfvén Wave Reflection

Bart van der Holst, G. Toth, I. Sokolov, W.B. Manchester, M. Jin, R. Oran, T.I. Gombosi

Center for Space Environment Modeling

University of Michigan

Outline

- BATS-R-US
- Alfvén wave turbulence driven corona and inner heliosphere model
- March 7, 2011 Coronal Mass Ejection (CME): 1T versus 2T
- Improved lower corona turbulence model with physics-based wave reflection
- Summary

The BATS-R-US Multiphysics Code

Time-stepping
Local explicit (CFL control) for steady state
Global explicit
Part steady explicit
Explicit/implicit
Point-implicit
Semi-implicit
Fully implicit

Conservation laws
Hydrodynamics, MHD
Ideal & non-ideal
Hall
Anisotropic pressure
Semi-relativistic
Multi-species
Multi-fluid
Ideal & non-ideal EOS

Numerics
Conservative finite-volume discretization
2nd (TVD), 4th (PPM) & 5th (MP) spatial order schemes
Rusanov/HLLE/AW/Roe/HLLD
Splitting the magnetic field into $B_0 + B_1$
Divergence B control
CT, 8-wave, projection, parabolic-hyperbolic cleaning

Block **A**daptive-**T**ree **S**olar-wind **R**oe-type **U**pwind **S**cheme

AMR Library (BATL)
Self-similar blocks
Cartesian grid
Curvilinear grid (can be stretched)
Supports 1, 2 and 3D block-adaptive grids
Allows AMR in a subset of the dimensions

Source terms
Gravity
Heat conduction
Ion-neutral friction
Ionization
Recombination
Charge exchange
Wave energy dissipation
Radiative heating/cooling

Auxiliary equations
Wave energy transport
Radiation transfer (multigroup diffusion)
Material interface (level set)
Parallel ray-tracing
Tabular equation of state

Alfvén Wave Solar Model (AWSoM)

- Inner boundary at T=50,000K (upper chromosphere)
- Density at inner boundary $n=2\times10^{17}$ m^{-3}
- The Alfvén wave Poynting flux at the inner boundary is proportional to the surface magnetic field:

  $S_A = V_A\, w = C\, B$

  where w is the Alfvén wave energy density at the inner boundary

  $C = (0.5 \div 1.5)\times10^{6}\ J\ m^{-2}\ s^{-1}\ T^{-1}$

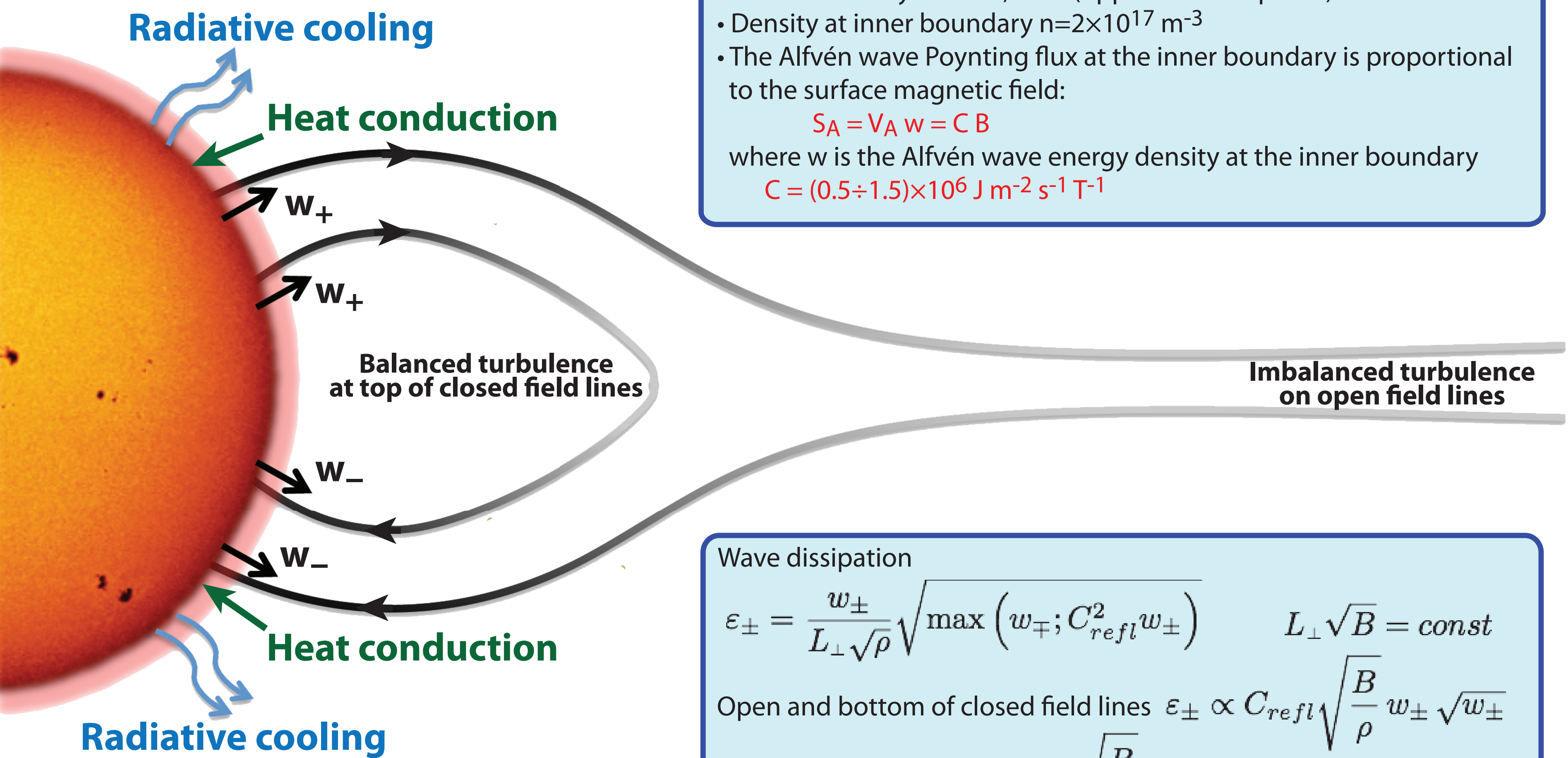

Wave dissipation

$$\varepsilon_\pm = \frac{w_\pm}{L_\perp\sqrt{\rho}}\sqrt{\max\left(w_\mp; C_{refl}^2 w_\pm\right)} \qquad L_\perp\sqrt{B} = const$$

Open and bottom of closed field lines $\varepsilon_\pm \propto C_{refl}\sqrt{\frac{B}{\rho}}\, w_\pm \sqrt{w_\pm}$

Top of closed field lines $\varepsilon_\pm \propto \sqrt{\frac{B}{\rho}}\, w_\pm \sqrt{w_\mp}$

Here $L_\perp$ is the perpendicular correlation length of Alfvénic turbulence

C_{refl} is a uniform reflection coefficient for wave mixing (0.01÷0.1)

Center for Space Environment Modeling
Space Weather Modeling Framework

Model Equations

$$\frac{\partial \rho}{\partial t} + \nabla \cdot (\rho \mathbf{u}) = 0$$

wave pressure gradient

$$\frac{\partial \rho \mathbf{u}}{\partial t} + \nabla \cdot \left(\rho \mathbf{u}\mathbf{u} + p_p + p_e + \frac{B^2}{2\mu_0} - \frac{\mathbf{B}\mathbf{B}}{\mu_0} + \frac{w_+ + w_-}{2} \right) = -\rho \frac{GM_\odot}{r^2}\mathbf{e}_r$$

$$\frac{\partial}{\partial t}\left(\frac{p_p}{\gamma - 1} + \frac{\rho u^2}{2} + \frac{B^2}{2\mu_0} \right) + \nabla \cdot \left[\left(\frac{\rho u^2}{2} + \frac{\gamma p_p}{\gamma - 1} + \frac{B^2}{\mu_0} \right) \mathbf{u} - \frac{\mathbf{B}(\mathbf{u}\cdot\mathbf{B})}{\mu_0} \right]$$

$$= -(\mathbf{u}\cdot\nabla)p_e + \frac{n_p k_B}{\tau_{pe}}(T_e - T_p) + (1-\alpha)(\Gamma_+ w_+ + \Gamma_- w_-) - \rho \mathbf{u}\cdot\mathbf{r}\frac{GM_\odot}{r^3}$$

collisional coupling

wave energy dissipation

$$\frac{\partial}{\partial t}\left(\frac{p_e}{\gamma - 1} \right) + \nabla \cdot \left(\frac{p_e}{\gamma - 1}\mathbf{u} \right) + p_e \nabla \cdot \mathbf{u}$$

$$= -\nabla \cdot \mathbf{q}_e + \frac{n_p k_B}{\tau_{pe}}(T_p - T_e) - n_p n_e \Lambda(T_e) + \alpha(\Gamma_+ w_+ + \Gamma_- w_-)$$

heat conduction

collisional coupling

radiative cooling

wave energy dissipation

$$\frac{\partial w_\pm}{\partial t} + \nabla \cdot (\mathbf{u} w_\pm \pm \mathbf{b} V_A w_\pm) + \frac{1}{2} w_\pm \nabla \cdot \mathbf{u} = -\Gamma_\pm w_\pm$$

wave energy dissipation

$$\Gamma_\pm = \frac{1}{L_\perp}\sqrt{\frac{\max\left(w_\mp\, ,\, C_{refl}^2 w_\pm\right)}{\rho}}$$

Model is driven by magnetogram input

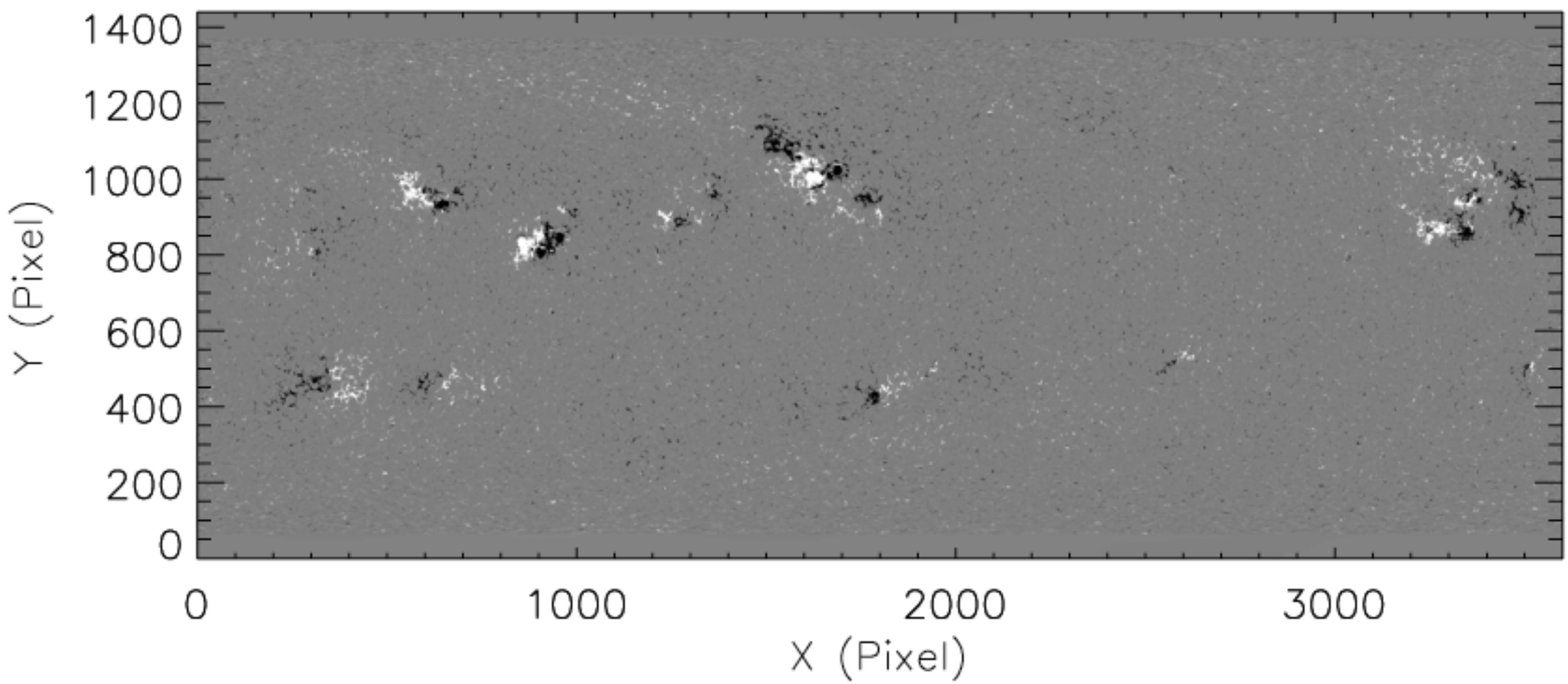

- Synoptic magnetogram of Carrington rotation 2107 from *SDO*/HMI. The saturation value of the magnetic field is set to be 200 G in order to show the active regions more clearly.

Computational Grids

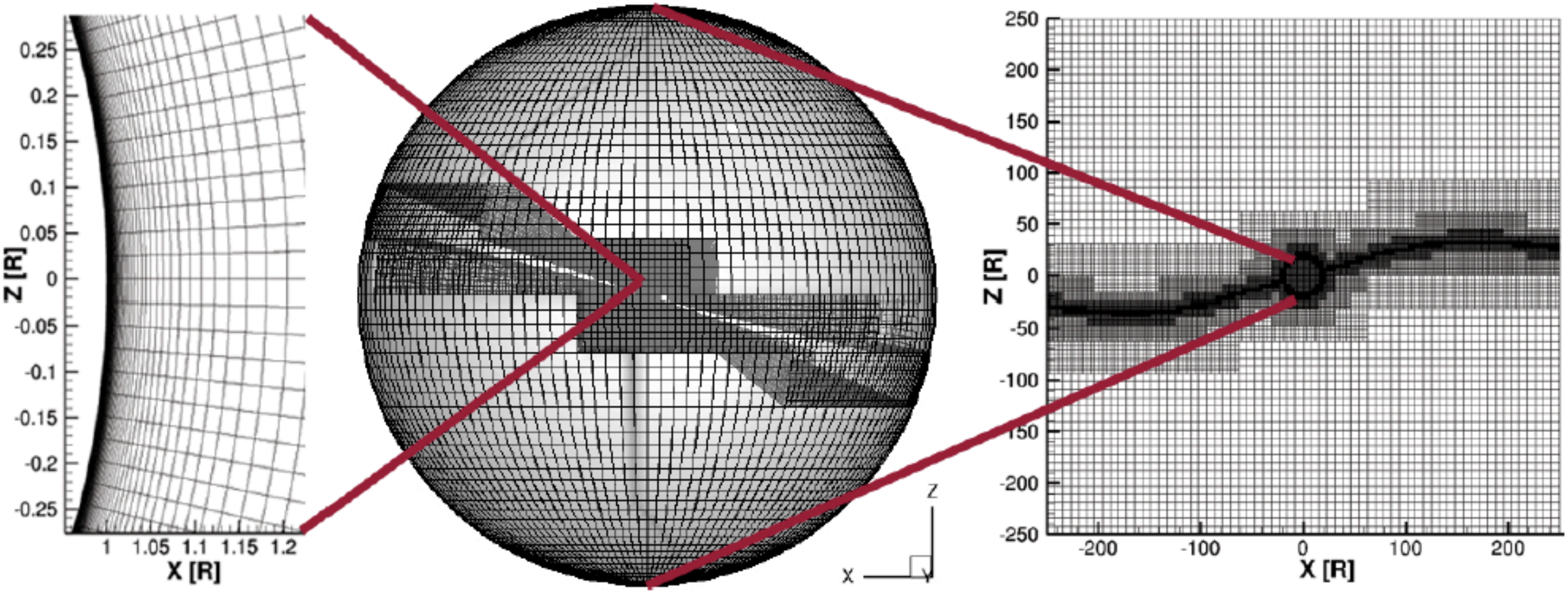

Solution for CR2107 (Feb-Mar 2011)

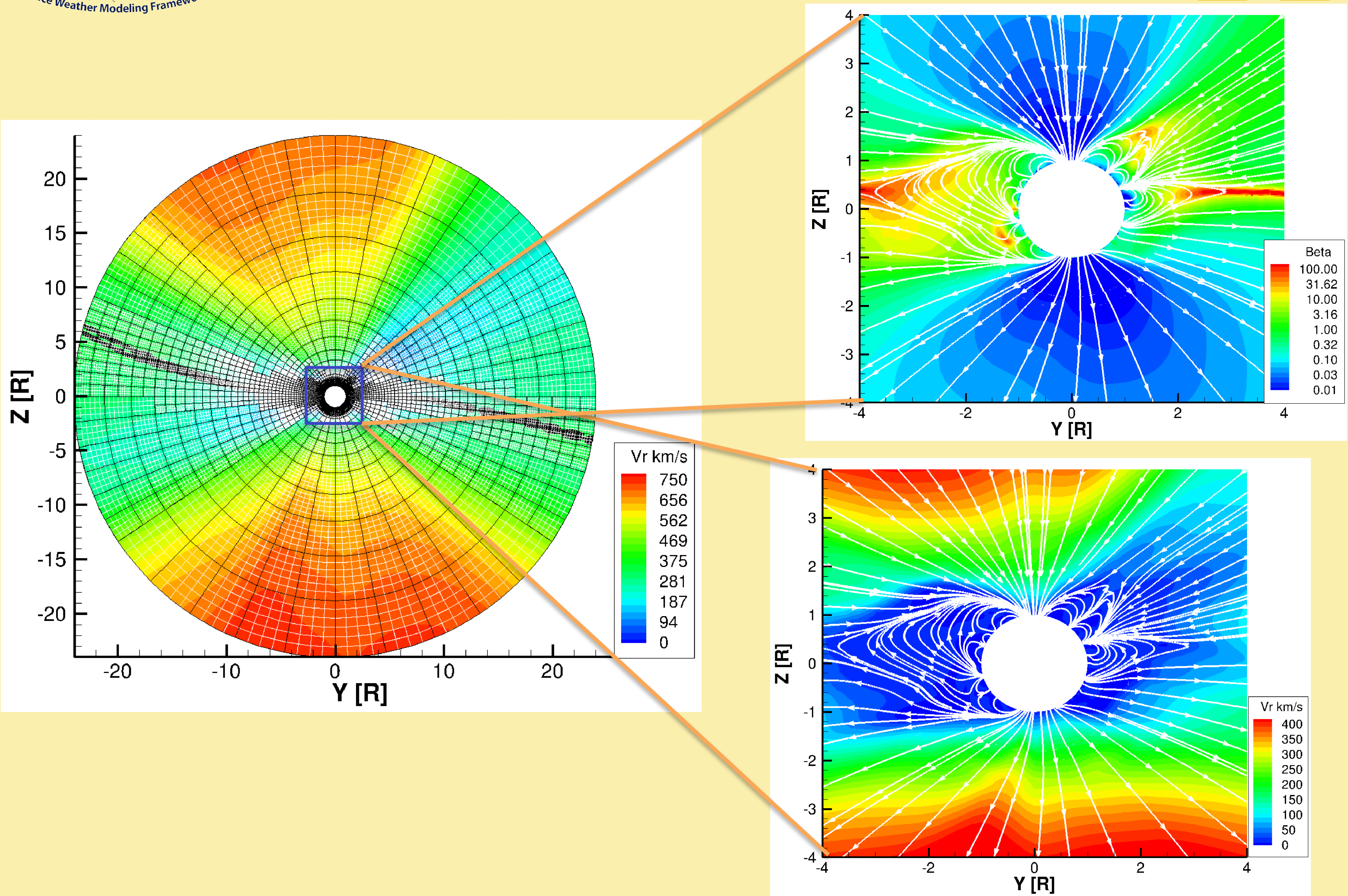

In-situ validation

Validation with WIND

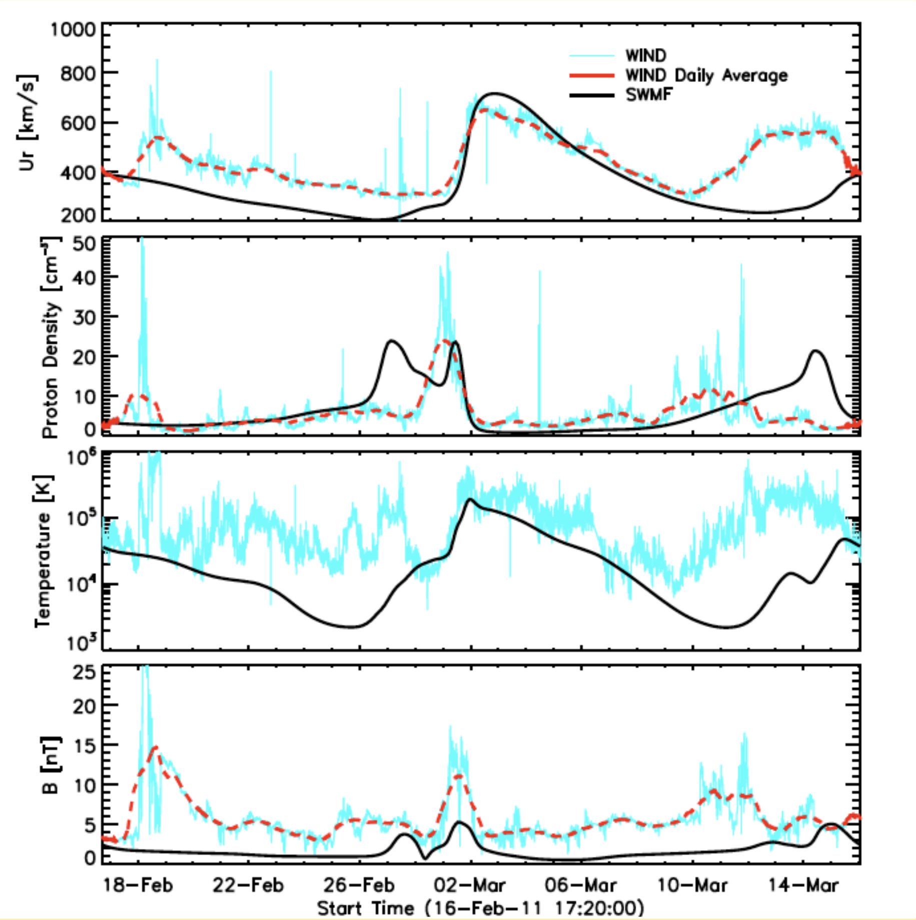

Validation with STEREO B

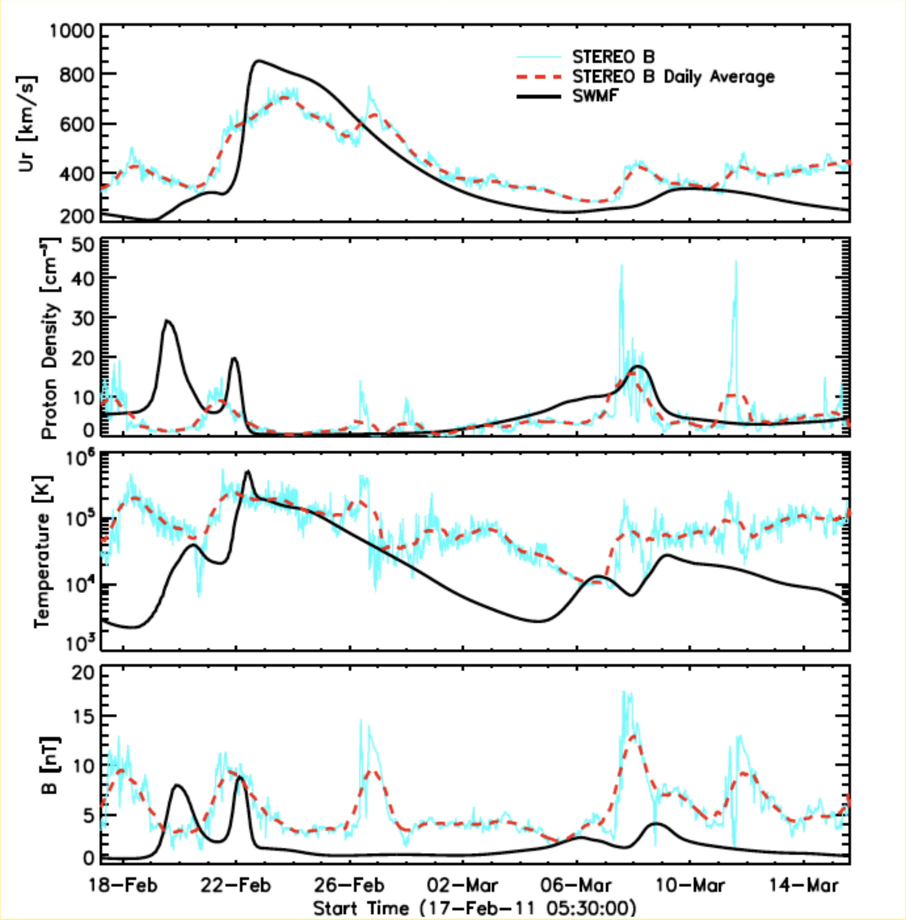

March 7, 2011 CME

AIA composite

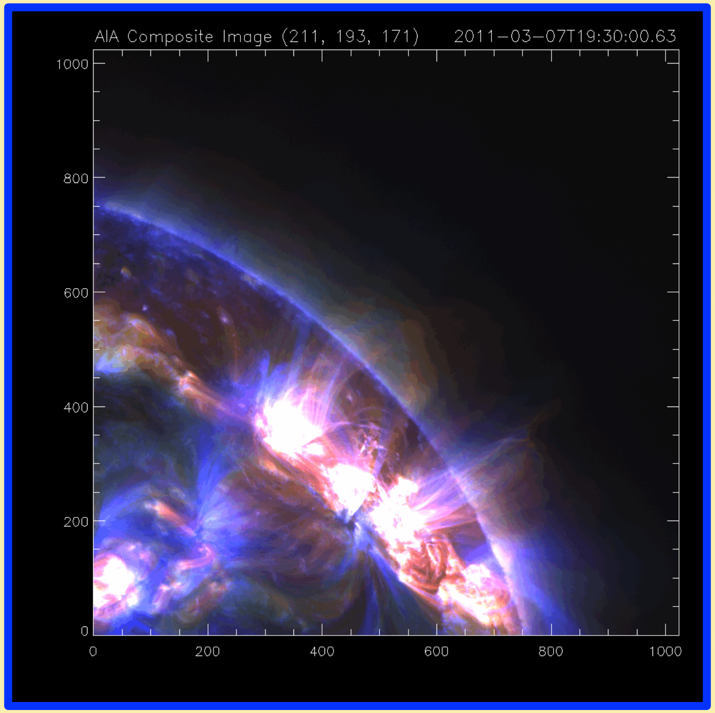

LASCO C2

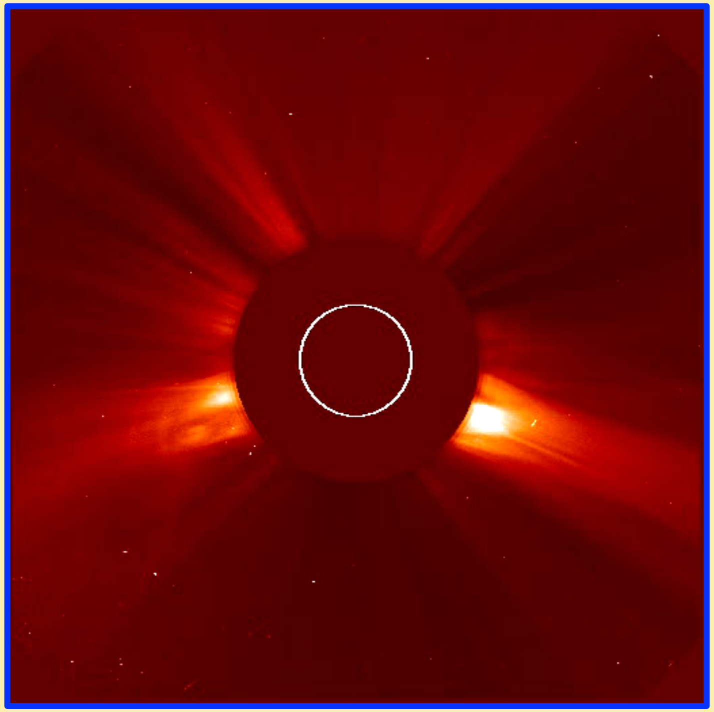

- **M3.7 Flare** occurred on March 7 (extended decay phase ~8 hrs).
- Followed by a very **fast CME** (~2200 km/s), **SEP event**, and **radio bursts**.

CME Initiation by Flux Rope Eruption

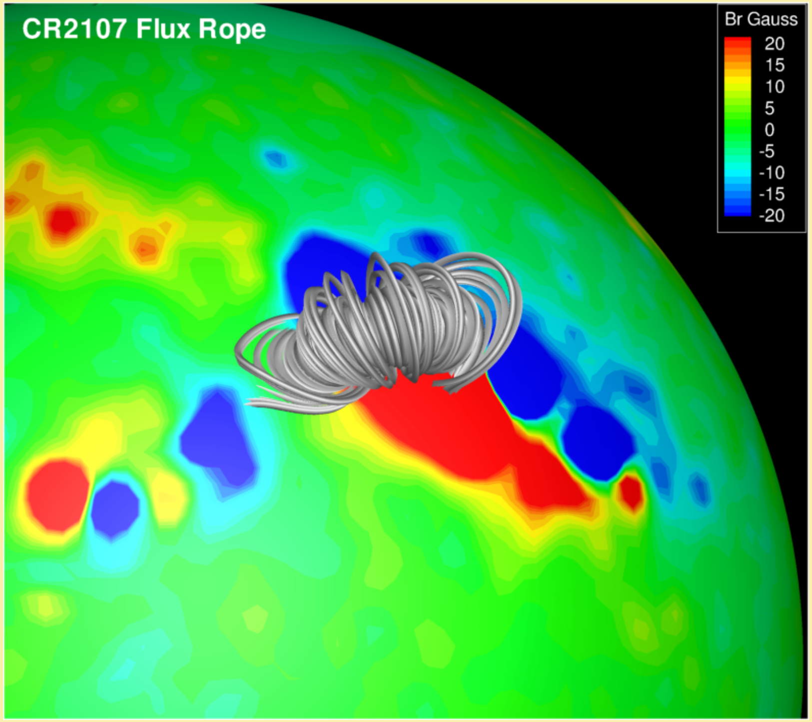

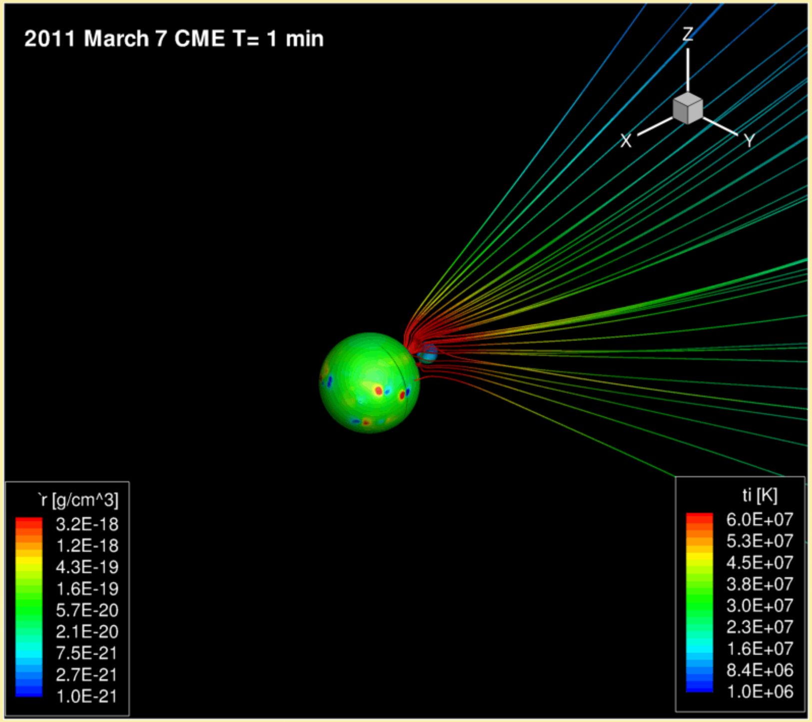

Analytical flux rope model first developed by *Titov & Demoulin (1999).*

$I = 2.0 \times 10^{12}$ A R = 60 Mm r= 9 Mm
Total Mass = 10^{16} g
Total Free Energy = 7.2×10^{33} ergs

V_r = 1000 km/s isosurface colored by proton temperature

1T or 2T ?

- The shock heating should only go to the protons due to the different sound speeds of electrons and protons (proton: ~100 km/s; electron: ~5000 km/s)
- In 1T the electron heat conduction also applies to protons. What are the consequences for the thermodynamics near the CME shock ?

1T and 2T CME Comparison

1T CME Temperature	2T CME Te	2T CME Tp

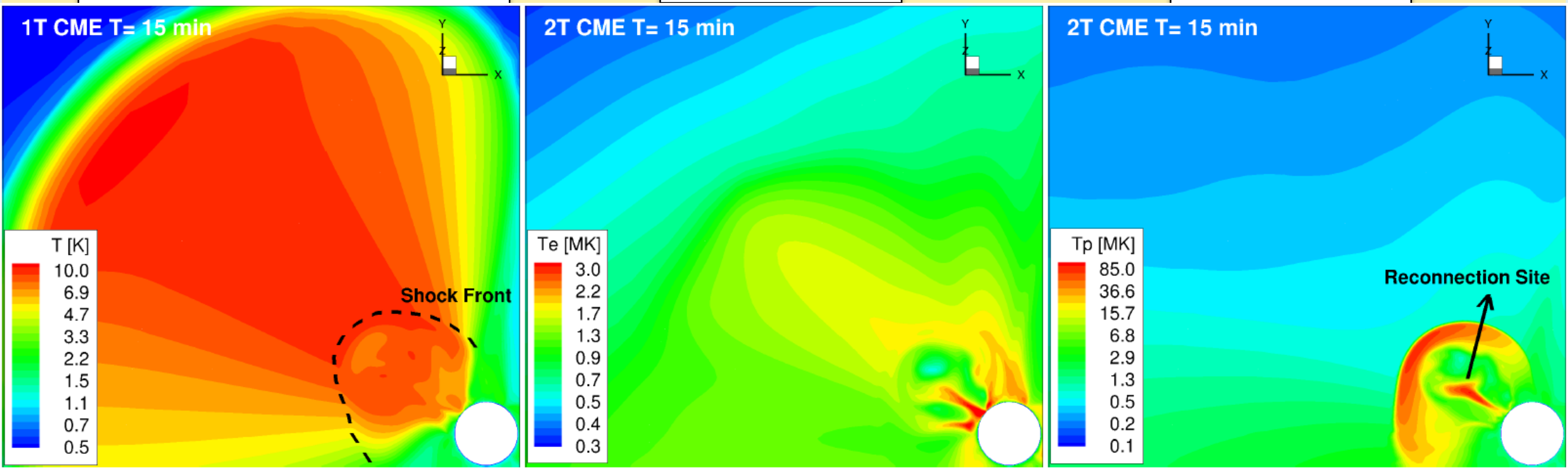

- In the 1T model, a strong **heat precursor** is in front of the CME, which is caused by the electron heat conduction applied to the proton temperature jump at the shock.
- In the 2T model, the strength of the heat precursor is much smaller than 1T case. At the shock the protons are heated to ~**85 MK**.

Compression Ratio Evolution

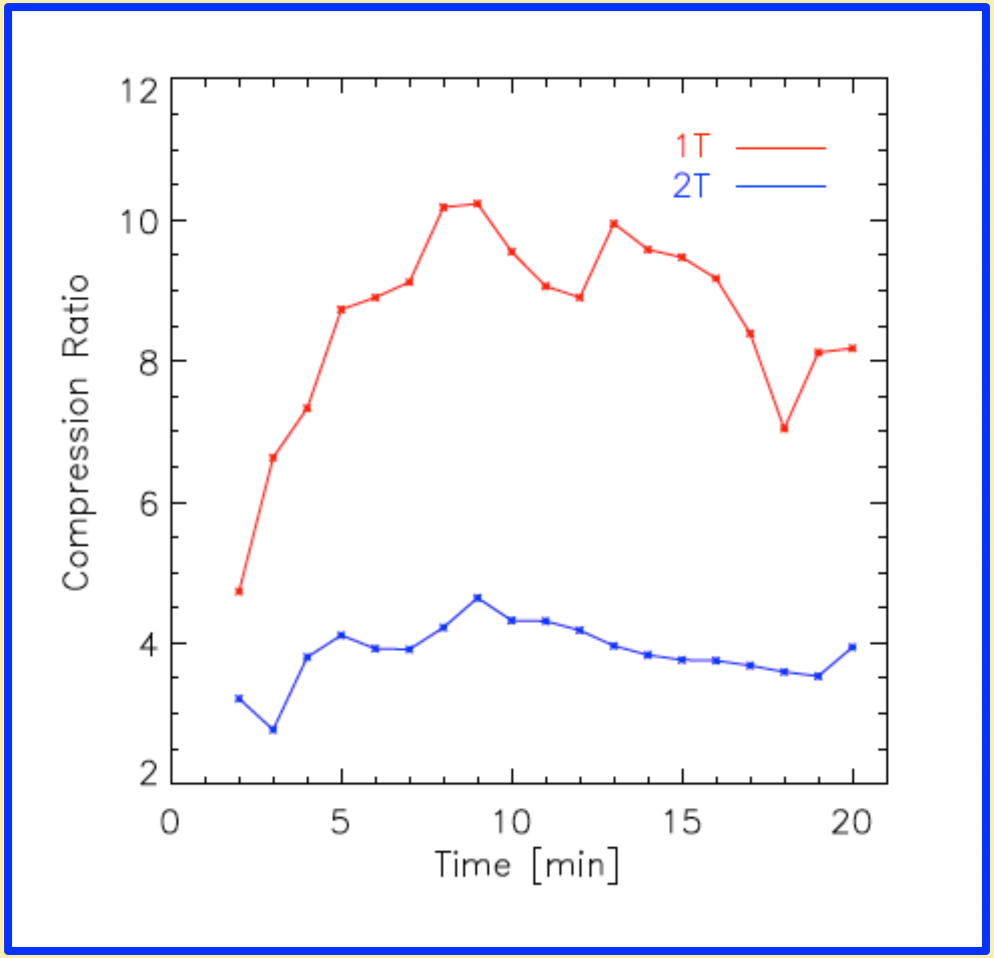

- For 1T CME, the compression ratio is always larger than 4 (hypersonic limit), with the maximum value reaches >10. (caused by unphysical heat conduction behind the shock that cools down the plasma efficiently and allows the density to increase.)
- For 2T CME, the compression ratio is around 4 during the whole evolution.

2T model is needed to produce correct properties of the CME-driven shocks.

Simulated White Light Images

Simulated LASCO C2

Observed LASCO C2

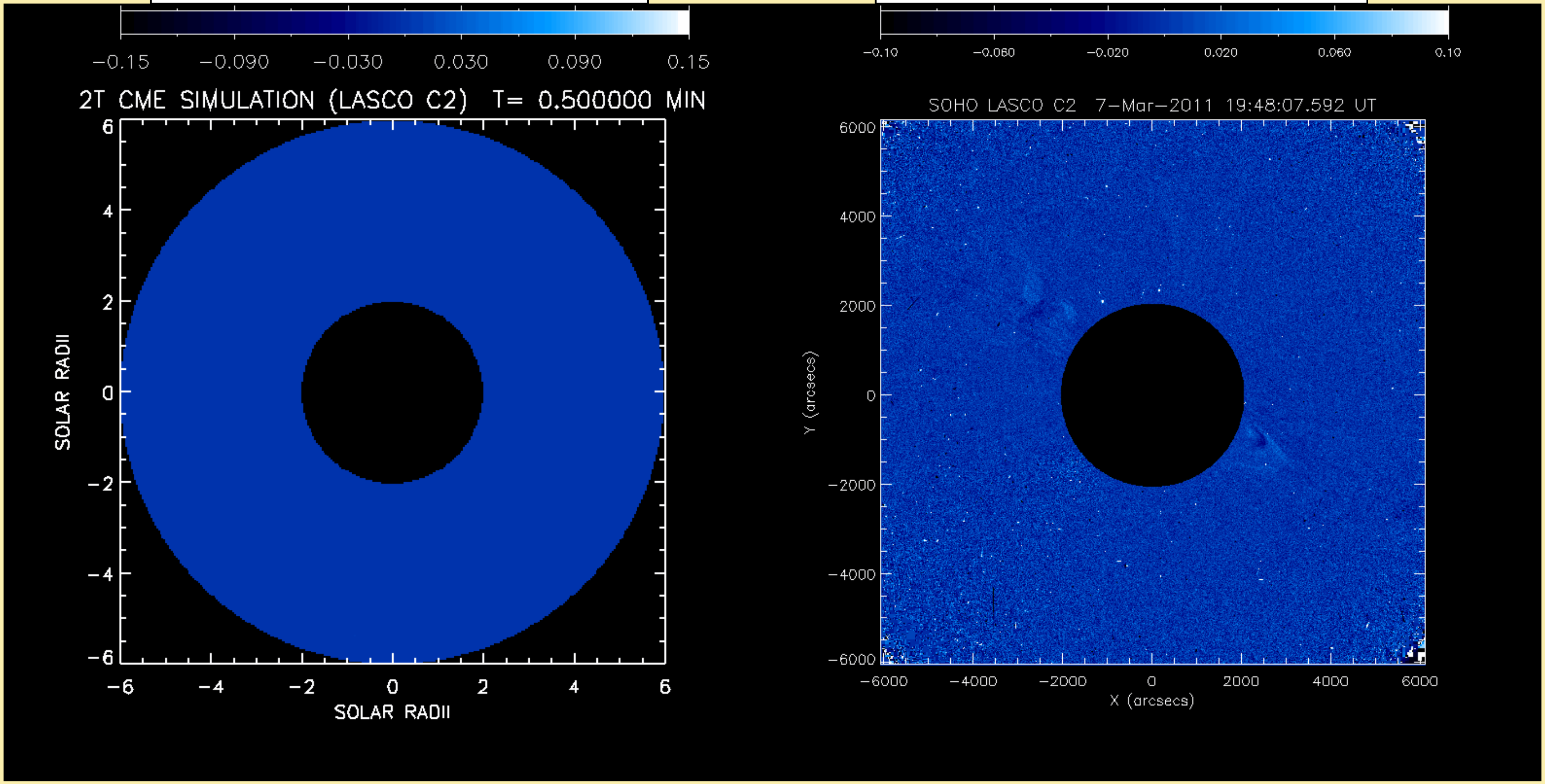

- **Typical double front morphology (Voulidas & Ontiveros, 2009) in which faint front is caused by shock and bright front is coronal plasma piled up at the top of the erupting flux rope**

Adaptive Mesh Refinement

Maximum Refinement Level 7

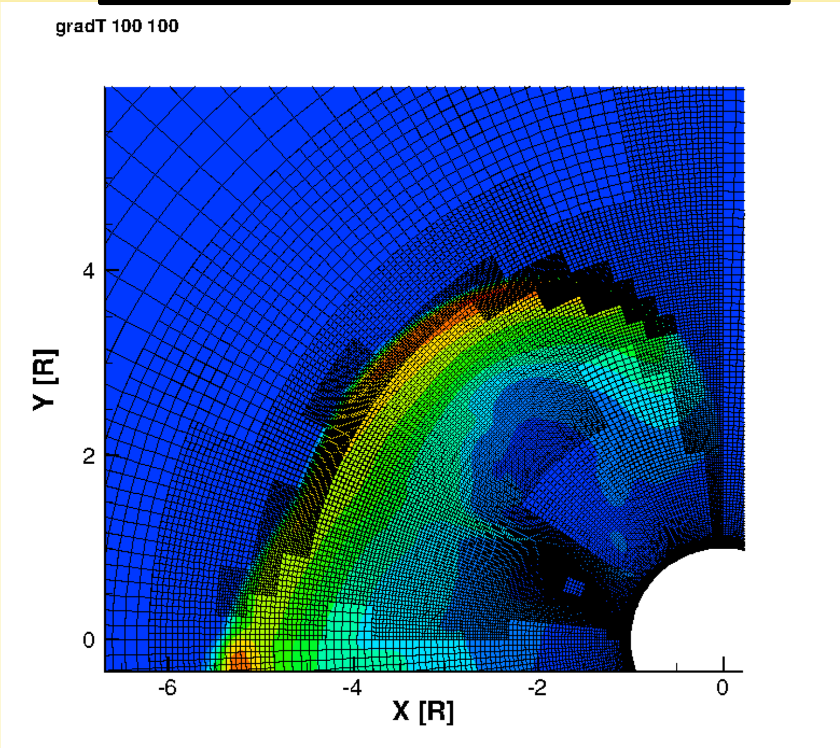

Maximum Refinement Level 8

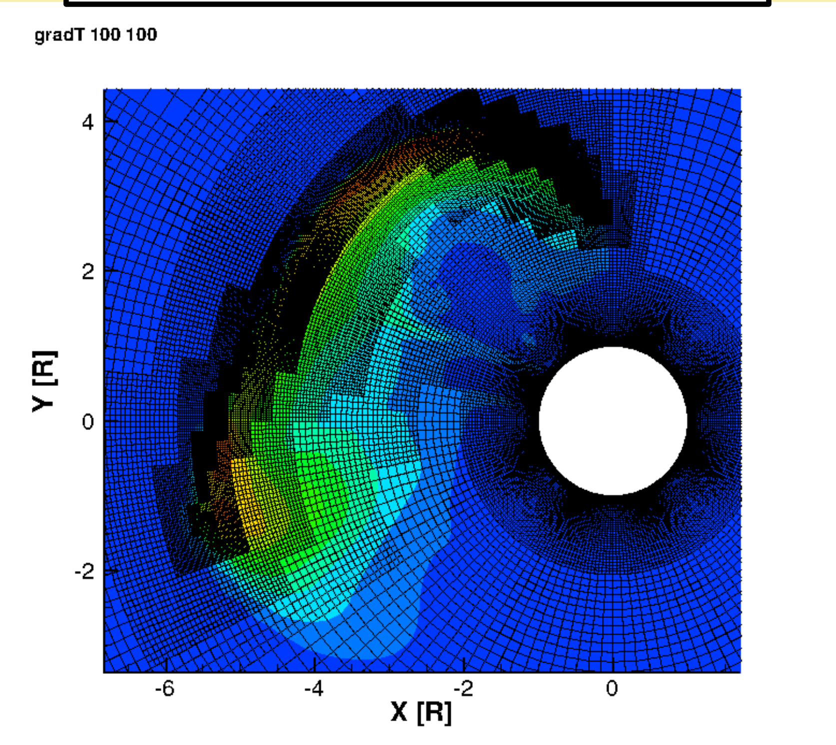

Proton temperature gradient criterion is reasonably good for shock refinement.

Need for coronal model improvements

- **Active regions are not as pronounced in the EUV images synthesized from simulations as in the observed images. What is missing in the lower corona model is enhanced wave reflected near active regions.**
- **We apply the following steps (see also e.g. Chandran et al., 2011, Li and Habbal, 2012):**
  - The nonlinear cascade is driven by partial reflection of outward propagating waves due to the gradients of the large-scale solar wind parameters
  - Amplitude of reflected inward propagating wave is much smaller than the outward propagating wave
  - Inward wave cascades sufficiently fast compared with their wave periods

Line-of-Sight Integrated Images
Stereo A, March 7 2011

New model (TVD) | New model (MP5) | Observation

171 Å
(1.0 MK)

195 Å
(1.4 MK)

284 Å
(2.2 MK)

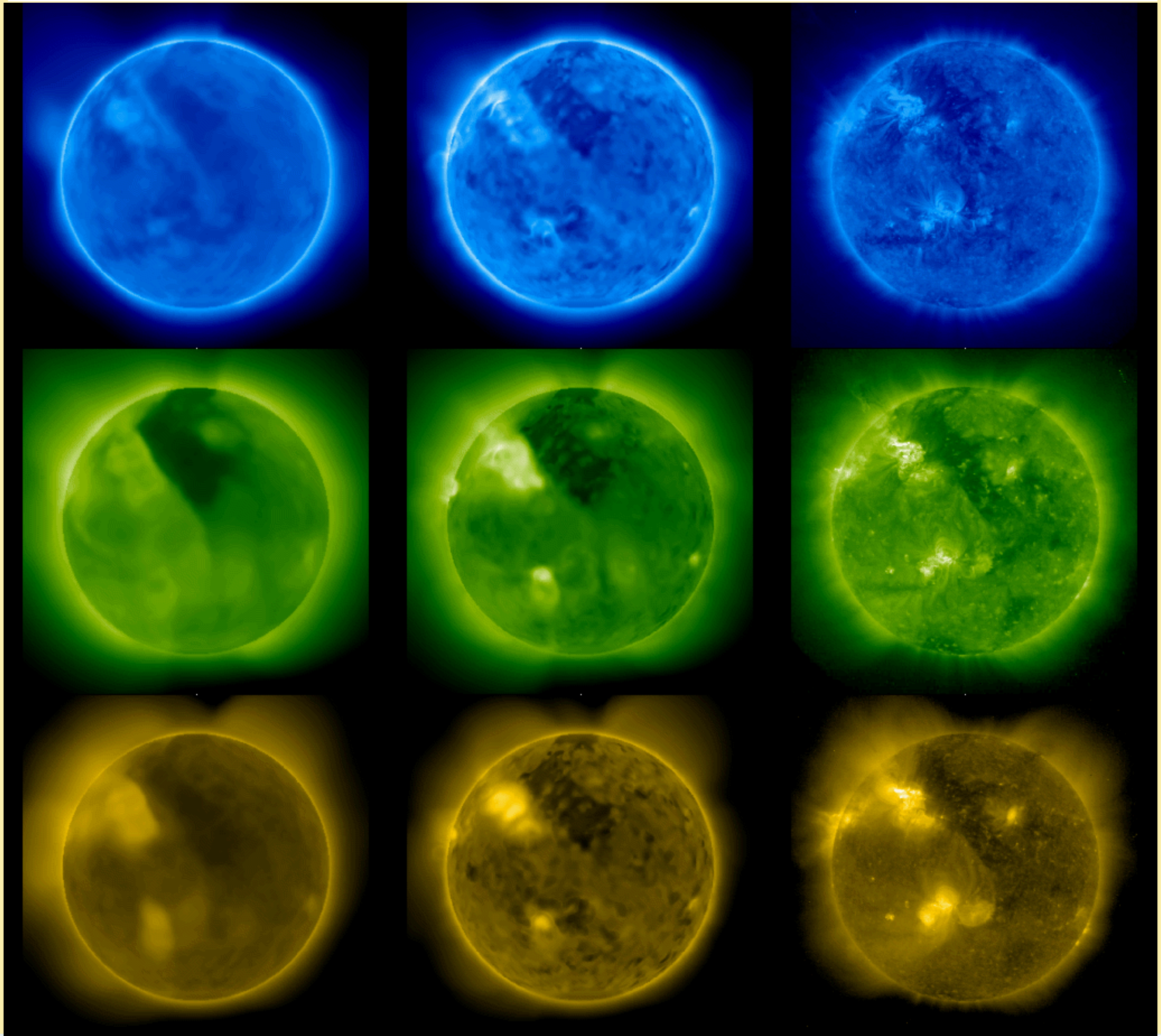

Line-of-Sight Integrated Images
Stereo A, March 7 2011

Old model (MP5) | New model (MP5) | Observation

171 Å (1.0 MK)

195 Å (1.4 MK)

284 Å (2.2 MK)

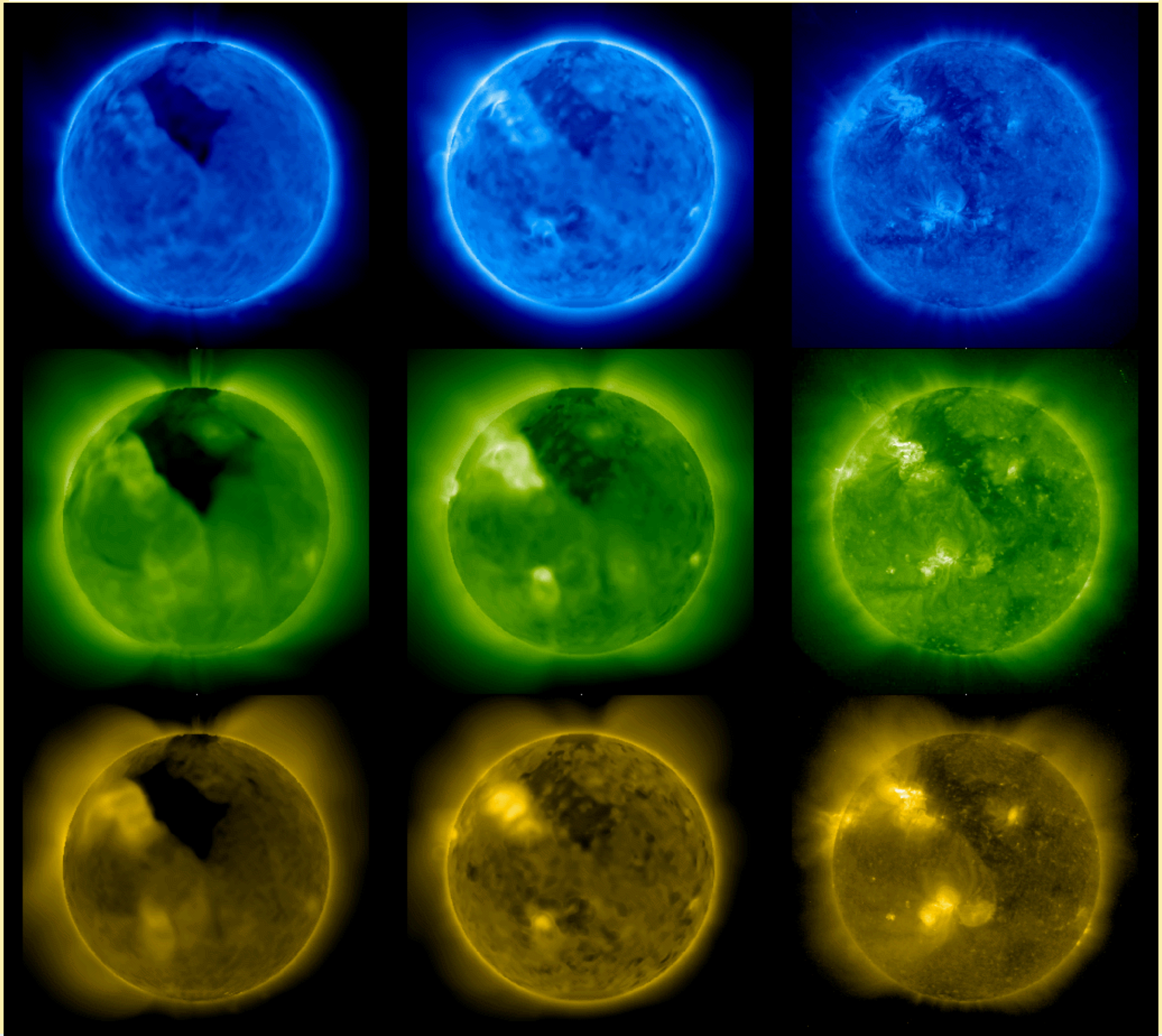

Line-of-Sight Integrated Images
Stereo B, March 7 2011

Old model (MP5) | New model (MP5) | Observation

171 Å (1.0 MK)

195 Å (1.4 MK)

284 Å (2.2 MK)

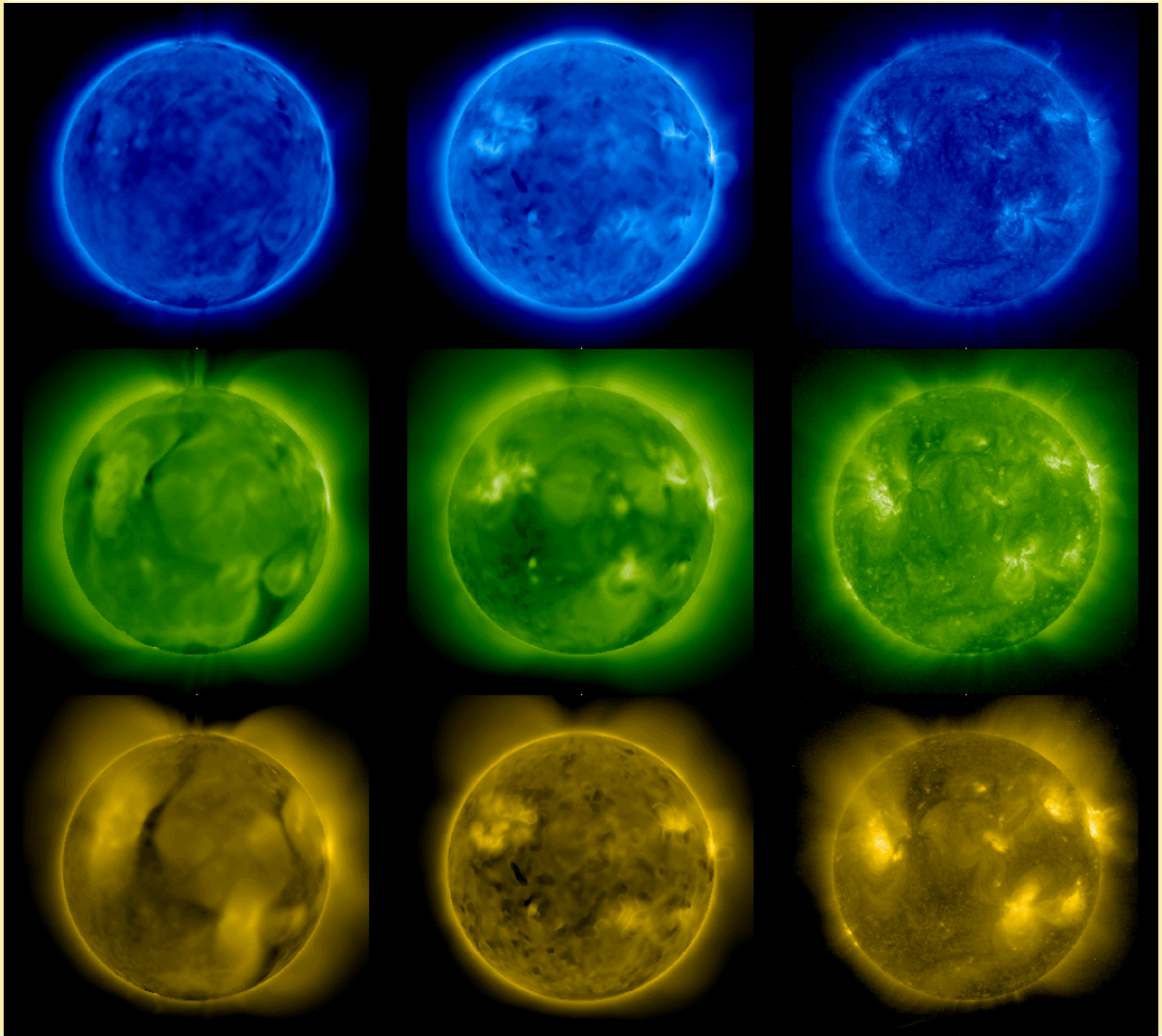

Summary

- **Previous two-temperature, Alfvén wave turbulence driven solar coronal and inner heliosphere model**
  - Inner boundary is in the upper chromosphere, outer boundary beyond Earth's orbit
  - Very small number of free parameters ($L_\perp$, C_{refl})
- **Validation with SOHO, STEREO, SDO, ACE and WIND**
- **2T CME simulations show proton shock heating**
- **1T simulations show unrealistic heat precursor and compression ratios**
- **New improved solar lower corona model**
  - Physics-based wave reflection
  - Simulated STEREO EUVI images start to resemble observations.
  - High order schemes help to resolve the details in these images.